Search for the sgoldstino at $\sqrt{s}$ from 189 to 202 GeV

P. Abreu, W. Adam, T. Adye, P. Adzic, Z. Albrecht, T. Alderweireld, G D. Alekseev, R. Alemany, T. Allmendinger, P P. Allport, et al.

EUROPEAN ORGANIZATION FOR NUCLEAR RESEARCH

CERN–EP/2000-110

16 August 2000

Search for the sgoldstino at $\sqrt{s}$ from 189 to 202 GeV

DELPHI Collaboration

Abstract

A search for the supersymmetric partner of the goldstino, the sgoldstino S, at LEP2 is presented. The production Sγ followed by S decay into two gluons or into two photons was studied at 189 - 202 GeV LEP centre-of-mass energies. No evidence for the S production was found and limits on the S mass corresponding to different theory parameters are given.

(Accepted by Phys.Lett.B)

P.Abreu[22], W.Adam[52], T.Adye[38], P.Adzic[12], Z.Albrecht[18], T.Alderweireld[2], G.D.Alekseev[17], R.Alemany[51], T.Allmendinger[18], P.P.Allport[23], S.Almehed[25], U.Amaldi[29], N.Amapane[47], S.Amato[49], E.Anashkin[37], E.G.Anassontzis[3], P.Andersson[46], A.Andreazza[28], S.Andringa[22], P.Antilogus[26], W-D.Apel[18], Y.Arnoud[15], B.Åsman[46], J-E.Augustin[24], A.Augustinus[9], P.Baillon[9], A.Ballestrero[47], P.Bambade[9,20], F.Barao[22], G.Barbiellini[48], R.Barbier[26], D.Y.Bardin[17], G.Barker[18], A.Baroncelli[40], M.Battaglia[16], M.Baubillier[24], K-H.Becks[54], M.Begalli[6], A.Behrmann[54], P.Beilliere[8], Yu.Belokopytov[9], N.C.Benekos[33], A.C.Benvenuti[5], C.Berat[15], M.Berggren[24], L.Berntzon[46], D.Bertrand[2], M.Besancon[41], M.S.Bilenky[17], M-A.Bizouard[20], D.Bloch[10], H.M.Blom[32], M.Bonesini[29], M.Boonekamp[41], P.S.L.Booth[23], G.Borisov[20], C.Bosio[43], O.Botner[50], E.Boudinov[32], B.Bouquet[20], C.Bourdarios[20], T.J.V.Bowcock[23], I.Boyko[17], I.Bozovic[12], M.Bozzo[14], M.Bracko[45], P.Branchini[40], R.A.Brenner[50], P.Bruckman[9], J-M.Brunet[8], L.Bugge[34], T.Buran[34], P.Buschmann[54], S.Cabrera[51], M.Caccia[28], M.Calvi[29], T.Camporesi[9], V.Canale[39], F.Carena[9], L.Carroll[23], C.Caso[14], M.V.Castillo Gimenez[51], A.Cattai[9], F.R.Cavallo[5], Ph.Charpentier[9], P.Checchia[37], G.A.Chelkov[17], R.Chierici[47], P.Chliapnikov[9,44], P.Chochula[7], V.Chorowicz[26], J.Chudoba[31], K.Cieslik[19], P.Collins[9], R.Contri[14], E.Cortina[51], G.Cosme[20], F.Cossutti[9], M.Costa[51], H.B.Crawley[1], D.Crennell[38], J.Croix[10], G.Crosetti[14], J.Cuevas Maestro[35], S.Czellar[16], J.D'Hondt[2], J.Dalmau[46], M.Davenport[9], W.Da Silva[24], G.Della Ricca[48], P.Delpierre[27], N.Demaria[47], A.De Angelis[48], W.De Boer[18], C.De Clercq[2], B.De Lotto[48], A.De Min[9], L.De Paula[49], H.Dijkstra[9], L.Di Ciaccio[39], J.Dolbeau[8], K.Doroba[53], M.Dracos[10], J.Drees[54], M.Dris[33], G.Eigen[4], T.Ekelof[50], M.Ellert[50], M.Elsing[9], J-P.Engel[10], M.Espirito Santo[9], G.Fanourakis[12], D.Fassouliotis[12], M.Feindt[18], J.Fernandez[42], A.Ferrer[51], E.Ferrer-Ribas[20], F.Ferro[14], A.Firestone[1], U.Flagmeyer[54], H.Foeth[9], E.Fokitis[33], F.Fontanelli[14], B.Franek[38], A.G.Frodesen[4], R.Fruhwirth[52], F.Fulda-Quenzer[20], J.Fuster[51], A.Galloni[23], D.Gamba[47], S.Gamblin[20], M.Gandelman[49], C.Garcia[51], C.Gaspar[9], M.Gaspar[49], U.Gasparini[37], Ph.Gavillet[9], E.N.Gazis[33], D.Gele[10], T.Geralis[12], N.Ghodbane[26], I.Gil[51], F.Glege[54], R.Gokieli[9,53], B.Golob[9,45], G.Gomez-Ceballos[42], P.Goncalves[22], I.Gonzalez Caballero[42], G.Gopal[38], L.Gorn[1], V.Gracco[14], J.Grahl[1], E.Graziani[40], P.Gris[41], G.Grosdidier[20], K.Grzelak[53], J.Guy[38], C.Haag[18], F.Hahn[9], S.Hahn[54], S.Haider[9], A.Hallgren[50], K.Hamacher[54], J.Hansen[34], F.J.Harris[36], F.Hauler[18], V.Hedberg[9,25], S.Heising[18], J.J.Hernandez[51], P.Herquet[2], H.Herr[9], E.Higon[51], S-O.Holmgren[46], P.J.Holt[36], S.Hoorelbeke[2], M.Houlden[23], J.Hrubec[52], M.Huber[18], G.J.Hughes[23], K.Hultqvist[9,46], J.N.Jackson[23], R.Jacobsson[9], P.Jalocha[19], R.Janik[7], Ch.Jarlskog[25], G.Jarlskog[25], P.Jarry[41], B.Jean-Marie[20], D.Jeans[36], E.K.Johansson[46], P.Jonsson[26], C.Joram[9], P.Juillot[10], L.Jungermann[18], F.Kapusta[24], K.Karafasoulis[12], S.Katsanevas[26], E.C.Katsoufis[33], R.Keranen[18], G.Kernel[45], B.P.Kersevan[45], B.A.Khomenko[17], N.N.Khovanski[17], A.Kiiskinen[16], B.King[23], A.Kinvig[23], N.J.Kjaer[9], O.Klapp[54], P.Kluit[32], P.Kokkinias[12], C.Kourkoumelis[3], O.Kouznetsov[17], M.Krammer[52], E.Kriznic[45], Z.Krumstein[17], P.Kubinec[7], J.Kurowska[53], K.Kurvinen[16], J.W.Lamsa[1], D.W.Lane[1], J-P.Laugier[41], R.Lauhakangas[16], G.Leder[52], F.Ledroit[15], L.Leinonen[46], A.Leisos[12], R.Leitner[31], J.Lemonne[2], G.Lenzen[54], V.Lepeltier[20], T.Lesiak[19], M.Lethuillier[26], J.Libby[36], W.Liebig[54], D.Liko[9], A.Lipniacka[46], I.Lippi[37], B.Loerstad[25], J.G.Loken[36], J.H.Lopes[49], J.M.Lopez[42], R.Lopez-Fernandez[15], D.Loukas[12], P.Lutz[41], L.Lyons[36], J.MacNaughton[52], J.R.Mahon[6], A.Maio[22], A.Malek[54], S.Maltezos[33], V.Malychev[17], F.Mandl[52], J.Marco[42], R.Marco[42], B.Marechal[49], M.Margoni[37], J-C.Marin[9], C.Mariotti[9], A.Markou[12], C.Martinez-Rivero[9], S.Marti i Garcia[9], J.Masik[13], N.Mastroyiannopoulos[12], F.Matorras[42], C.Matteuzzi[29], G.Matthiae[39], F.Mazzucato[37], M.Mazzucato[37], M.Mc Cubbin[23], R.Mc Kay[1], R.Mc Nulty[23], G.Mc Pherson[23], E.Merle[15], C.Meroni[28], W.T.Meyer[1], E.Migliore[9], L.Mirabito[26], W.A.Mitaroff[52], U.Mjoernmark[25], T.Moa[46], M.Moch[18], R.Moeller[30], K.Moenig[9,11], M.R.Monge[14], J.Montenegro[32], D.Moraes[49], G.Morton[36], U.Mueller[54], K.Muenich[54], M.Mulders[32], C.Mulet-Marquis[15], L.M.Mundim[6], R.Muresan[25], W.J.Murray[38], B.Muryn[19], G.Myatt[36], T.Myklebust[34], F.Naraghi[15], M.Nassiakou[12], F.L.Navarria[5], K.Nawrocki[53], P.Negri[29], N.Neufeld[52], R.Nicolaidou[41], B.S.Nielsen[30], P.Niezurawski[53], M.Nikolenko[10,17], V.Nomokonov[16], A.Nygren[25], A.G.Olshevski[17], A.Onofre[22], R.Orava[16], K.Osterberg[9], A.Ouraou[41], A.Oyanguren[51], M.Paganoni[29], S.Paiano[5], R.Pain[24], R.Paiva[22], J.Palacios[36], H.Palka[19], Th.D.Papadopoulou[33], L.Pape[9], C.Parkes[9], F.Parodi[14], U.Parzefall[23], A.Passeri[40], O.Passon[54], T.Pavel[25], M.Pegoraro[37], L.Peralta[22], M.Pernicka[52], A.Perrotta[5], C.Petridou[48], A.Petrolini[14], H.T.Phillips[38], F.Pierre[41], M.Pimenta[22], E.Piotto[28], T.Podobnik[45], V.Poireau[41], M.E.Pol[6], G.Polok[19], P.Poropat[48], V.Pozdniakov[17], P.Privitera[39], N.Pukhaeva[17], A.Pullia[29], D.Radojicic[36], S.Ragazzi[29], H.Rahmani[33], J.Rames[13], P.N.Ratoff[21], A.L.Read[34], P.Rebecchi[9], N.G.Redaelli[29], M.Regler[52], J.Rehn[18], D.Reid[32], P.Reinertsen[4], R.Reinhardt[54], P.B.Renton[36], L.K.Resvanis[3], F.Richard[20], J.Ridky[13], G.Rinaudo[47], I.Ripp-Baudot[10], A.Romero[47], P.Ronchese[37], E.I.Rosenberg[1], P.Rosinsky[7], P.Roudeau[20], T.Rovelli[5], V.Ruhlmann-Kleider[41], A.Ruiz[42], H.Saarikko[16], Y.Sacquin[41], A.Sadovsky[17], G.Sajot[15], J.Salt[51], D.Sampsonidis[12], M.Sannino[14], A.Savoy-Navarro[24], C.Schwanda[52], Ph.Schwemling[24], B.Schwering[54], U.Schwickerath[18], F.Scuri[48], P.Seager[21], Y.Sedykh[17], A.M.Segar[36], N.Seibert[18], R.Sekulin[38], G.Sette[14], R.C.Shellard[6], M.Siebel[54], L.Simard[41], F.Simonetto[37], A.N.Sisakian[17], G.Smadja[26], O.Smirnova[25], G.R.Smith[38], A.Sopczak[18], R.Sosnowski[53], T.Spassov[9], E.Spiriti[40], S.Squarcia[14], C.Stanescu[40], M.Stanitzki[18], K.Stevenson[36], A.Stocchi[20], J.Strauss[52], R.Strub[10], B.Stugu[4], M.Szczekowski[53], M.Szeptycka[53], T.Tabarelli[29], A.Taffard[23], F.Tegenfeldt[50], F.Terranova[29], J.Timmermans[32], N.Tinti[5], L.G.Tkatchev[17], M.Tobin[23], S.Todorova[9], B.Tome[22], A.Tonazzo[9], L.Tortora[40], P.Tortosa[51], G.Transtromer[25], D.Treille[9], G.Tristram[8], M.Trochimczuk[53], C.Troncon[28], M-L.Turluer[41], I.A.Tyapkin[17], P.Tyapkin[25], S.Tzamarias[12], O.Ullaland[9], G.Valenti[9,5], E.Vallazza[48], C.Vander Velde[2], P.Van Dam[32], W.Van den Boeck[2], W.K.Van Doninck[2], J.Van Eldik[9,32], A.Van Lysebetten[2], N.van Remortel[2],

I.Van Vulpen[32], G.Vegni[28], L.Ventura[37], W.Venus[38,9], F.Verbeure[2], P.Verdier[26], M.Verlato[37], L.S.Vertogradov[17], V.Verzi[28], D.Vilanova[41], L.Vitale[48], A.S.Vodopyanov[17], G.Voulgaris[3], V.Vrba[13], H.Wahlen[54], A.J.Washbrook[23], C.Weiser[9], D.Wicke[9], J.H.Wickens[2], G.R.Wilkinson[36], M.Winter[10], M.Witek[19], G.Wolf[9], J.Yi[1], A.Zalewska[19], P.Zalewski[53], D.Zavrtanik[45], E.Zevgolatakos[12], N.I.Zimin[17,25], A.Zintchenko[17], Ph.Zoller[10], G.Zumerle[37], M.Zupan[12]

[1]Department of Physics and Astronomy, Iowa State University, Ames IA 50011-3160, USA
[2]Physics Department, Univ. Instelling Antwerpen, Universiteitsplein 1, B-2610 Antwerpen, Belgium
and IIHE, ULB-VUB, Pleinlaan 2, B-1050 Brussels, Belgium
and Faculté des Sciences, Univ. de l'Etat Mons, Av. Maistriau 19, B-7000 Mons, Belgium
[3]Physics Laboratory, University of Athens, Solonos Str. 104, GR-10680 Athens, Greece
[4]Department of Physics, University of Bergen, Allégaten 55, NO-5007 Bergen, Norway
[5]Dipartimento di Fisica, Università di Bologna and INFN, Via Irnerio 46, IT-40126 Bologna, Italy
[6]Centro Brasileiro de Pesquisas Físicas, rua Xavier Sigaud 150, BR-22290 Rio de Janeiro, Brazil
and Depto. de Física, Pont. Univ. Católica, C.P. 38071 BR-22453 Rio de Janeiro, Brazil
and Inst. de Física, Univ. Estadual do Rio de Janeiro, rua São Francisco Xavier 524, Rio de Janeiro, Brazil
[7]Comenius University, Faculty of Mathematics and Physics, Mlynska Dolina, SK-84215 Bratislava, Slovakia
[8]Collège de France, Lab. de Physique Corpusculaire, IN2P3-CNRS, FR-75231 Paris Cedex 05, France
[9]CERN, CH-1211 Geneva 23, Switzerland
[10]Institut de Recherches Subatomiques, IN2P3 - CNRS/ULP - BP20, FR-67037 Strasbourg Cedex, France
[11]Now at DESY-Zeuthen, Platanenallee 6, D-15735 Zeuthen, Germany
[12]Institute of Nuclear Physics, N.C.S.R. Demokritos, P.O. Box 60228, GR-15310 Athens, Greece
[13]FZU, Inst. of Phys. of the C.A.S. High Energy Physics Division, Na Slovance 2, CZ-180 40, Praha 8, Czech Republic
[14]Dipartimento di Fisica, Università di Genova and INFN, Via Dodecaneso 33, IT-16146 Genova, Italy
[15]Institut des Sciences Nucléaires, IN2P3-CNRS, Université de Grenoble 1, FR-38026 Grenoble Cedex, France
[16]Helsinki Institute of Physics, HIP, P.O. Box 9, FI-00014 Helsinki, Finland
[17]Joint Institute for Nuclear Research, Dubna, Head Post Office, P.O. Box 79, RU-101 000 Moscow, Russian Federation
[18]Institut für Experimentelle Kernphysik, Universität Karlsruhe, Postfach 6980, DE-76128 Karlsruhe, Germany
[19]Institute of Nuclear Physics and University of Mining and Metalurgy, Ul. Kawiory 26a, PL-30055 Krakow, Poland
[20]Université de Paris-Sud, Lab. de l'Accélérateur Linéaire, IN2P3-CNRS, Bât. 200, FR-91405 Orsay Cedex, France
[21]School of Physics and Chemistry, University of Lancaster, Lancaster LA1 4YB, UK
[22]LIP, IST, FCUL - Av. Elias Garcia, 14-1^{o}, PT-1000 Lisboa Codex, Portugal
[23]Department of Physics, University of Liverpool, P.O. Box 147, Liverpool L69 3BX, UK
[24]LPNHE, IN2P3-CNRS, Univ. Paris VI et VII, Tour 33 (RdC), 4 place Jussieu, FR-75252 Paris Cedex 05, France
[25]Department of Physics, University of Lund, Sölvegatan 14, SE-223 63 Lund, Sweden
[26]Université Claude Bernard de Lyon, IPNL, IN2P3-CNRS, FR-69622 Villeurbanne Cedex, France
[27]Univ. d'Aix - Marseille II - CPP, IN2P3-CNRS, FR-13288 Marseille Cedex 09, France
[28]Dipartimento di Fisica, Università di Milano and INFN-MILANO, Via Celoria 16, IT-20133 Milan, Italy
[29]Dipartimento di Fisica, Univ. di Milano-Bicocca and INFN-MILANO, Piazza delle Scienze 2, IT-20126 Milan, Italy
[30]Niels Bohr Institute, Blegdamsvej 17, DK-2100 Copenhagen Ø, Denmark
[31]IPNP of MFF, Charles Univ., Areal MFF, V Holesovickach 2, CZ-180 00, Praha 8, Czech Republic
[32]NIKHEF, Postbus 41882, NL-1009 DB Amsterdam, The Netherlands
[33]National Technical University, Physics Department, Zografou Campus, GR-15773 Athens, Greece
[34]Physics Department, University of Oslo, Blindern, NO-1000 Oslo 3, Norway
[35]Dpto. Fisica, Univ. Oviedo, Avda. Calvo Sotelo s/n, ES-33007 Oviedo, Spain
[36]Department of Physics, University of Oxford, Keble Road, Oxford OX1 3RH, UK
[37]Dipartimento di Fisica, Università di Padova and INFN, Via Marzolo 8, IT-35131 Padua, Italy
[38]Rutherford Appleton Laboratory, Chilton, Didcot OX11 OQX, UK
[39]Dipartimento di Fisica, Università di Roma II and INFN, Tor Vergata, IT-00173 Rome, Italy
[40]Dipartimento di Fisica, Università di Roma III and INFN, Via della Vasca Navale 84, IT-00146 Rome, Italy
[41]DAPNIA/Service de Physique des Particules, CEA-Saclay, FR-91191 Gif-sur-Yvette Cedex, France
[42]Instituto de Fisica de Cantabria (CSIC-UC), Avda. los Castros s/n, ES-39006 Santander, Spain
[43]Dipartimento di Fisica, Università degli Studi di Roma La Sapienza, Piazzale Aldo Moro 2, IT-00185 Rome, Italy
[44]Inst. for High Energy Physics, Serpukov P.O. Box 35, Protvino, (Moscow Region), Russian Federation
[45]J. Stefan Institute, Jamova 39, SI-1000 Ljubljana, Slovenia and Laboratory for Astroparticle Physics,
Nova Gorica Polytechnic, Kostanjeviska 16a, SI-5000 Nova Gorica, Slovenia,
and Department of Physics, University of Ljubljana, SI-1000 Ljubljana, Slovenia
[46]Fysikum, Stockholm University, Box 6730, SE-113 85 Stockholm, Sweden
[47]Dipartimento di Fisica Sperimentale, Università di Torino and INFN, Via P. Giuria 1, IT-10125 Turin, Italy
[48]Dipartimento di Fisica, Università di Trieste and INFN, Via A. Valerio 2, IT-34127 Trieste, Italy
and Istituto di Fisica, Università di Udine, IT-33100 Udine, Italy
[49]Univ. Federal do Rio de Janeiro, C.P. 68528 Cidade Univ., Ilha do Fundão BR-21945-970 Rio de Janeiro, Brazil
[50]Department of Radiation Sciences, University of Uppsala, P.O. Box 535, SE-751 21 Uppsala, Sweden
[51]IFIC, Valencia-CSIC, and D.F.A.M.N., U. de Valencia, Avda. Dr. Moliner 50, ES-46100 Burjassot (Valencia), Spain
[52]Institut für Hochenergiephysik, Österr. Akad. d. Wissensch., Nikolsdorfergasse 18, AT-1050 Vienna, Austria
[53]Inst. Nuclear Studies and University of Warsaw, Ul. Hoza 69, PL-00681 Warsaw, Poland
[54]Fachbereich Physik, University of Wuppertal, Postfach 100 127, DE-42097 Wuppertal, Germany

1 Introduction

In the Supersymmetric extension of the Standard Model, once Supersymmetry is spontaneously broken the gravitino $\tilde{\mathrm{G}}$ can acquire a mass by absorbing the degrees of freedom of the goldstino. This mechanism is analogous to the spontaneous breaking of the electro-weak symmetry in the Standard Model, where the Z and W bosons acquire mass by absorbing the goldstone bosons.

A light gravitino as predicted by some supersymmetric models [1] has been searched for at LEP and Tevatron experiments [2,3]. Limits on the $\tilde{\mathrm{G}}$ mass allow lower limits on the supersymmetry-breaking scale $\sqrt{F}$ to be inferred.

Recently it has been pointed out [4] that an appropriate theory must contain also the supersymmetric partner of the goldstino, called the sgoldstino, which could be massive. The production of this particle may be relevant at present LEP energies if the supersymmetry-breaking scale and the sgoldstino mass are not too large. In the minimal R-parity-conserving model, as considered in [4], the effective theory at the weak scale contains two neutral scalar states: the S which is CP-even, and the P which is CP-odd. As sgoldstinos have even R parity, they are not necessarily produced in pairs and their decay chains do not necessarily contain an LSP (Lightest Supersymmetric Particle). The phenomenology of these two particles is similar. The following formulae and results will be expressed for the S state but are valid also for the P particle.

At LEP 2, one of the most interesting production channels is the process $e^+e^- \rightarrow S\gamma$, which depends on the S mass m_S and on $\sqrt{F}$:

$$\frac{d\sigma}{dcos\theta}(e^+e^- \rightarrow S\gamma) = \frac{|\Sigma|^2\, s}{64\pi F^2}\left(1-\frac{m_S^2}{s}\right)^3 (1+cos^2\theta), \tag{1}$$

where θ is the scattering angle in the centre-of-mass and

$$|\Sigma|^2 = \frac{e^2 M_{\gamma\gamma}^2}{2s} + \frac{g_Z^2(v_e^2+a_e^2)M_{\gamma Z}^2 s}{2(s-m_Z^2)^2} + \frac{e g_Z v_e M_{\gamma\gamma} M_{\gamma Z}}{s-m_Z^2} \tag{2}$$

with $v_e = sin^2\theta_W - 1/4$, $a_e = 1/4$ and $g_Z = e/(sin\theta_W cos\theta_W)$. $M_{\gamma\gamma}$ and $M_{\gamma Z}$ are related to the diagonal mass terms for the $U(1)_Y$ and $SU(2)_L$ gauginos M_1 and M_2:

$$M_{\gamma\gamma} = M_1 cos^2\theta_W + M_2 sin^2\theta_W,\ M_{\gamma Z} = (M_2 - M_1) sin\theta_W cos\theta_W. \tag{3}$$

The most relevant S decay modes are $S \rightarrow \gamma\gamma$ and $S \rightarrow gg$ with

$$\Gamma(S \rightarrow \gamma\gamma) = \frac{m_S^3 M_{\gamma\gamma}^2}{32\pi F^2} \tag{4}$$

and

$$\Gamma(S \rightarrow gg) = \frac{m_S^3 M_3^2}{4\pi F^2}, \tag{5}$$

where M_3 is the gluino mass. The corresponding branching ratios depend on M_1, M_2 and M_3, and the total width is $\Gamma \sim \Gamma(S \rightarrow \gamma\gamma) + \Gamma(S \rightarrow gg)$. In this letter two sets for these parameters as suggested in [4] are considered and listed in Table 1.

For a large interval of the parameter space the total width is small (below a few GeV/c^2), except for the region with small $\sqrt{F}$ where the production cross section is also expected to be very large.

The two decay channels considered produce events with very different topologies:

	M_1	M_2	M_3	B.R. $S \to \gamma\gamma$	B.R. $S \to gg$
1)	200	300	400	4%	96%
2)	350	350	350	11%	89%

Table 1: Two choices for the gaugino mass parameters (in GeV/c^2) relevant for the sgoldstino production and decay and the corresponding Branching Ratios of the two considered channels.

1. $S \to \gamma\gamma$ gives rise to events with three high energy photons, one of which is expected to be monochromatic with energy $E_\gamma = \frac{s-m_S^2}{2\sqrt{s}}$ for the large fraction of the parameter space where S has a negligible width. Despite its lower branching ratio (4 and 11% for the two sets of Table 1, respectively), this final state is worth investigating because the main background source is the QED process $e^+e^- \to \gamma\gamma(\gamma)$, which is expected to be small if photons in the forward region are discarded.
2. $S \to gg$ gives rise to events with one monochromatic photon (except for the region with small $\sqrt{F}$) and two jets. An irreducible background from $e^+e^- \to q\bar{q}\gamma$ events is associated to this topology. Therefore the signal must be searched for as an excess of events over the background expectation for every mass hypothesis.

This letter describes the results obtained with the DELPHI detector at LEP centre-of-mass energies of 189, 192, 196, 200 and 202 GeV, corresponding to a total integrated luminosity of about 380 pb^{-1}.

2 Apparatus

A detailed description of the DELPHI detector can be found in [5]. The present analysis was mainly based on the measurement of the electromagnetic energy clusters [6] in the barrel electromagnetic calorimeter, the High density Projection Chamber (HPC), and in the Forward ElectroMagnetic Calorimeter (FEMC), as well as on the capability of reconstructing charged particle tracks using the tracking devices: the Vertex Detector (VD), the Inner Detector (ID), the Time Projection Chamber (TPC), the Outer Detector (OD) and the forward chambers (FCA and FCB). The Vertex Detector [7] extends its coverage down to 10.5° in polar angle θ. An electromagnetic calorimeter (STIC) was used to measure the luminosity.

The barrel and the forward electromagnetic energy triggers were based on data from the HPC and the FEMC respectively. The calorimetric trigger efficiency for $e^+e^- \to \gamma\gamma(\gamma)$ was estimated with samples of Bhabha $e^+e^- \to e^+e^-(\gamma)$ events. This was done by counting how often the electromagnetic trigger was fired by an electron which had been triggered by an independent track trigger. In events with more than two photons, as well as in events with photons and charged particle tracks, the trigger efficiency was better than 99%.

3 Event selection and analysis

The 1998 data were taken at $\sqrt{s}$ = 188.6 GeV, and the 1999 data at 191.6, 195.5, 199.5 and 201.6 GeV. The integrated luminosities obtained requiring the HPC, FEMC,

TPC and VD to be operational were 155.1 pb^{-1}, 25.1 pb^{-1}, 76.2 pb^{-1}, 83.1 pb^{-1} and 40.1 pb^{-1} respectively for the five centre-of-mass energies.

Monte-Carlo generated events for the same centre-of-mass energies were processed through the full DELPHI simulation [5] and the same reconstruction chain as real data.

3.1 $S \to \gamma\gamma$ channel

Events were selected as $\gamma\gamma\gamma$ candidates if they had:

- at least two electromagnetic energy clusters with $0.219 < E/\sqrt{s} < 0.713$;
- at least one additional cluster with $E > 5$ GeV and no more than two additional clusters, of which the second one (if present) had $E < 5$ GeV;
- the two most energetic electromagnetic clusters in the HPC region $42^\circ < \theta < 89^\circ$ or in the FEMC region $25^\circ < \theta < 32.4^\circ$;
- the third cluster in the region $42^\circ < \theta$ or $20^\circ < \theta < 35^\circ$;
- no hits in two of the three Vertex Detector layers within $\pm 2^\circ$ in azimuthal angle ϕ of the line from the mean beam crossing point to any electromagnetic cluster.

Further, two hemispheres were defined by a plane orthogonal to the direction of the most energetic cluster. One hemisphere was required to have no charged particle detected in the barrel region of the detector with momentum above 1 GeV/c extrapolating to within 5 cm of the mean beam crossing point. The requirement was strengthened, to suppress the large e^+e^- background further, by demanding that both hemispheres have no such particle detected by the TPC with $\theta < 35^\circ$.

The events selected have a three-body final state kinematics if no significant additional radiation is lost in the detector (mainly initial state radiation lost along the beam pipe). A simple way to check if an event is, within a reasonable approximation, a three-body final state, is to look at the distribution of the quantity $\Delta = |\delta_{12}| + |\delta_{13}| + |\delta_{23}|$ where δ_{ij} is the angle between the particle i and j (Fig. 1). In a three-body final state, the particles lie in a plane and therefore Δ should be 360°. If only the events with $\Delta > 358^\circ$ are accepted, the energies of the particles can be determined with very good precision from their measured directions:

$$E_1 = \sqrt{s}\frac{sin\delta_{23}}{\delta};\ E_2 = \sqrt{s}\frac{sin\delta_{13}}{\delta};\ E_3 = \sqrt{s}\frac{sin\delta_{12}}{\delta} \tag{6}$$

with $\delta = sin\delta_{12}+sin\delta_{13}+sin\delta_{23}$. The error on the energy evaluation was further minimised by requiring $min(\delta_{12}, \delta_{13}, \delta_{23}) > 2^\circ$.

In $S\gamma$ events, the S decay products are isotropically distributed in the S centre-of-mass system. The distribution of $cos\alpha$, where α is the angle between the S direction (opposite to the prompt photon) and the direction of one of the two S decay products, in the S centre-of-mass system, should therefore be flat. On the other hand, in the QED background $|cos\alpha|$ peaks at 1. Therefore, out of the three combinations present in each event, only those giving $|cos\alpha| < 0.9$ were accepted.

The numbers of selected events, each giving up to three combinations, are listed with the expected background in Table 2. No significant background was found except for the QED process $e^+e^- \to \gamma\gamma(\gamma)$.

The acceptance for an $S\gamma$ signal produced according to (1) after the described polar angle cuts was $(51 \pm 2)\%$. The dependence on m_S from 10 to 190 GeV/c^2 was contained within the error quoted. The selection efficiency inside the acceptance region was evaluated by means of the QED background events generated according to [8], The efficiency

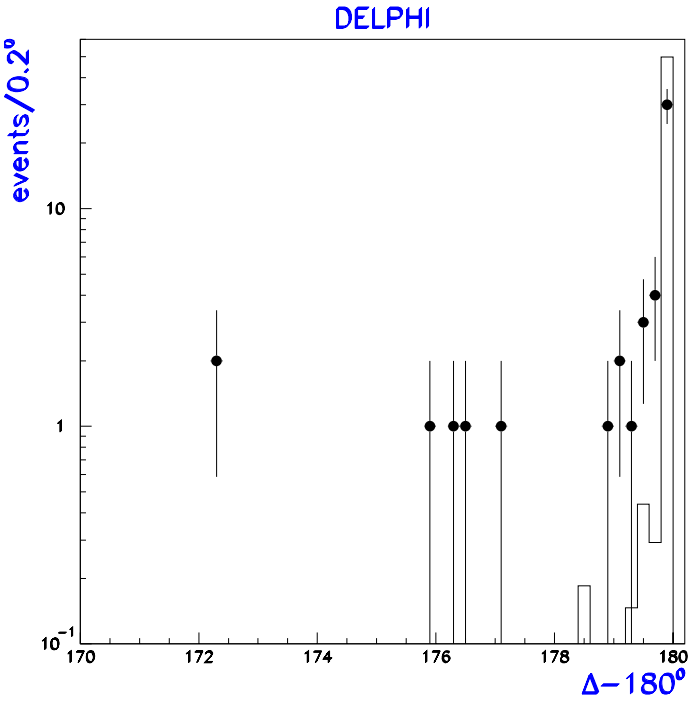

Figure 1: $\Delta - 180^0$ for the $\gamma\gamma\gamma$ candidates (points) and the QED $e^+e^- \to \gamma\gamma(\gamma)$ simulated sample (histogram). The cuts on $min(\delta_{12}, \delta_{13}, \delta_{23}) > 2^\circ$ and on $cos\alpha$ are not applied in this figure.

was independent, within the errors, of the photon polar angle. Its average value was $(76.6 \pm 2.5)\%$.

The energy resolution obtained from (6) was also evaluated using simulated QED events as shown in Fig.2. It was better than 0.5 % in the whole photon energy range: a fit with two Gaussians gave two resolution components with $\sigma_1 = 0.12$ GeV and $\sigma_2 = 0.35$ GeV with about equal frequencies.

The second component was introduced to describe the tails originating from photons detected near the calorimeter dead regions.

3.2 $S \to gg$ channel

This channel is expected to give rise to a final state with one photon and two jets. An event was selected as a γgg candidate if it had:

- an electromagnetic energy cluster identified as a photon with $E > 5$ GeV and $\theta > 20^\circ$;
- no electromagnetic cluster with $\theta < 5^\circ$;
- total multiplicity greater than 10;
- charged particle multiplicity greater than 5;
- $\sqrt{\sum_{i=1}^{n}(p_x^2 + p_y^2)_i} > 0.12 \times \sqrt{s}$, where n is the total multiplicity;
- the sum of the absolute values of all particle momenta along the thrust axis greater than $0.20 \times \sqrt{s}$;

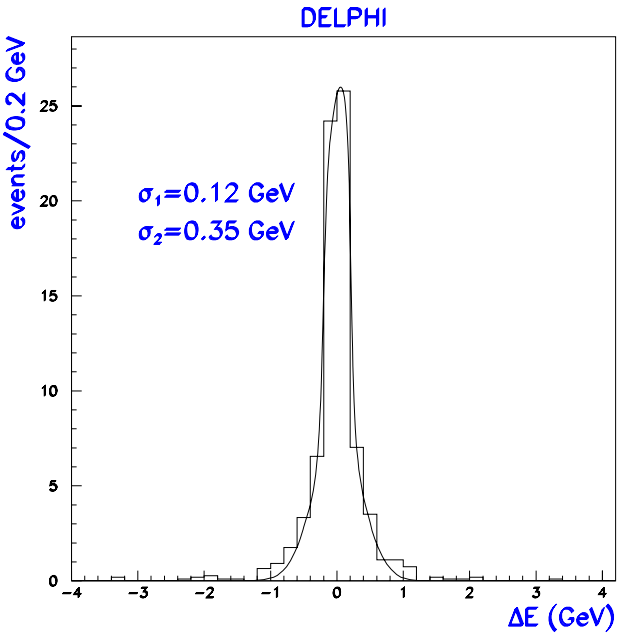

Figure 2: The energy resolution ΔE for the photons of the $\gamma\gamma\gamma$ candidates in the QED $e^+e^- \to \gamma\gamma(\gamma)$ simulated sample. The photon energy was obtained using (6). A fit with two Gaussians gave two resolution components $\sigma_1 = 0.12$ GeV and $\sigma_2 = 0.35$ GeV with approximately equal frequencies.

- either an electromagnetic cluster with $E < 0.45 \times \sqrt{s}$, or a total multiplicity greater than 16 if the cluster energy is greater than $0.45 \times \sqrt{s}$;
- $|cos(\theta_p)| < 0.995$, where θ_p is the polar angle of the missing momentum;
- visible energy greater than $0.60 \times \sqrt{s}$;
- $|\cos\alpha| < 0.9$;
- Δ greater than $350°$.

The events were reconstructed forcing all particles but the photon into a 2-jet topology using the DURHAM [10] algorithm. Events were removed if $y_{cut} > 0.02$ and if the angle between the photon and the nearest jet was less than $10°$. If the event contained more than one photon candidate, the most energetic one was considered as the one produced in $e^+e^- \to S\gamma$. In addition, the jets were required to be incompatible with the $b\bar{b}$ hypothesis by requiring the combined btag of the events to be less than zero [9].

As in the $\gamma\gamma\gamma$ selection, the events obtained after this selection are three-body final state events in the absence of additional lost radiation. Therefore all the kinematic constraints described in the previous subsection were also applied here. In this case, however, as jet directions are less precisely determined than photons directions, the cut in Δ was less stringent and the resolution for the reconstructed photon energy was poorer: a two-Gaussian fit gave $\sigma_1 = 1.2$ GeV (55% of the area) and $\sigma_2 = 4.1$ GeV.

The polar angle acceptance for an $S\gamma$ signal produced according to (1) was $(76 \pm 2\%)$ and almost independent of m_S. The selection efficiency inside the acceptance region was evaluated using the $q\bar{q}\gamma$ background events generated with PYTHIA [11], processed through the full DELPHI analysis chain and re-weighted according to the background

and signal photon polar angle distributions. It ranged from 20 to 55 % depending on the photon energy.

In addition to the main background from $q\bar{q}\gamma$ events, a small (less than 5%) fraction was due to four-fermion processes which were generated according to EXCALIBUR [12]. The numbers of selected events and the expected background are listed in Table 2.

channel	$\sqrt{s}$ (GeV)	events	background
$S \to \gamma\gamma$	189	11	19 ± 2
$S \to \gamma\gamma$	192 to 202	19	24^{-2}_{+3}
$S \to g\ g$	189	771	782 ± 24
$S \to g\ g$	192	113	113 ± 3
$S \to g\ g$	196	339	316 ± 5
$S \to g\ g$	200	342	330 ± 6
$S \to g\ g$	202	169	158 ± 3

Table 2: Number of selected events for the two decay channels and expected number of background events. The background for the $S \to \gamma\gamma$ channel is dominated by the QED process $e^+e^- \to \gamma\gamma(\gamma)$, for the $S \to g\ g$ channel by the process $e^+e^- \to q\bar{q}\gamma$. The errors include systematic effects (see text).

4 Results

The photon recoil mass spectra obtained for the two decay channels are shown in Fig. 3 and Fig. 4. The data are superimposed on the expected background distributions. In the case of the $S \to \gamma\gamma$ channel, the QED background generator included corrections only to order α^3 and therefore no additional radiation was simulated. Additional radiation tends to give rise to a tail of events having low values of Δ (Fig. 1). These events were removed only from the selected sample of real data, and therefore a corresponding normalisation correction of $(-13^{+4}_{-7})\%$ was applied to the simulated sample. This correction was the dominant contribution to the systematic uncertainty for the $S \to \gamma\gamma$ channel.

In the case of the $S \to gg$ channel, the systematic error was due to the Monte-Carlo statistics and to the uncertainty on the luminosity determination, which was 0.56% for the 1998 data and 1.0% for the 1999 data. The $e^+e^- \to q\bar{q}\gamma$ background for the 189 GeV data was generated with PYTHIA version 5.722, which did not accurately reproduce the angular distribution of the radiative photon. Therefore the Monte-Carlo events at that energy were corrected on the basis of the ratio between events generated at higher energies according to PYTHIA version 5.722 and PYTHIA version 6.125. The systematic error on the number of expected events at 189 GeV includes the uncertainty in this correction.

No excess of events and no clear evidence of anomalous production of events with monochromatic photons is observed in either channel. Therefore a limit on the cross section of the new physics reaction contributing to the two topologies was set.

The number of detected events, the background rate and the detection efficiency depend on the S mass hypothesis considered. In addition, when the expected total width for a given m_S value is comparable with the experimental resolution or larger, the data were compared with the background events in a region corresponding to 80% of the signal area. As a consequence, the limit on the signal cross section depends on both m_S and $\sqrt{F}$. To take into account the different sensitivities of the two analysed channels, the

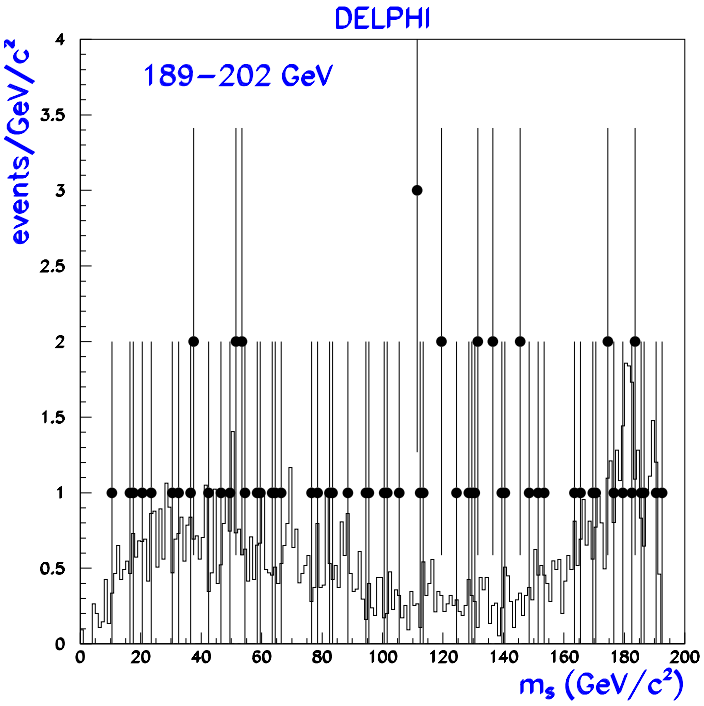

Figure 3: Photon recoil mass spectrum for the $\gamma\gamma\gamma$ candidates (points) and the expected background (histogram). The average number of entries per event in the data is 2.3. The bin size takes into account the experimental mass resolution and the expected signal width.

likelihood ratio method was used [13]. Since the expected S branching ratio and total width depend on the mass parameters, as explained above, the 95% Confidence Level cross section limit was computed as a function of m_S and $\sqrt{F}$ for the two sets of parameters listed in Table 1. The result is shown in Fig. 5. By comparing the experimental limits with the production cross section computed from (1), it is possible to determine a 95% Confidence Level excluded region of the parameter space. This is shown in Fig. 6. As explained in [4], to keep the particle interpretation the total width Γ must be much smaller than m_S and therefore the region with $\Gamma > 0.5 \times m_S$ was not considered. The 95% Confidence Level limits on the cross section times branching ratio for the two decay channels are given in Fig. 7. They are obtained for $\sqrt{F} \geq 500$ GeV, corresponding to the region where the expected signal width is independent of $\sqrt{F}$ as it is dominated by the experimental resolution.

5 Conclusions

The first search for the production of $S\gamma$ ($P\gamma$) where S (P) is a CP-even (CP-odd) state of the sgoldstino, the goldstino supersymmetric partner, was made using the data collected by DELPHI at LEP in 1998 and 1999 at centre-of-mass energies from 189 to 202 GeV for a total integrated luminosity of about 380 pb^{-1}. The $\gamma\gamma\gamma$ and γgg final states expected from $S(P) \to \gamma\gamma$ and $S(P) \to gg$ production and decay respectively,

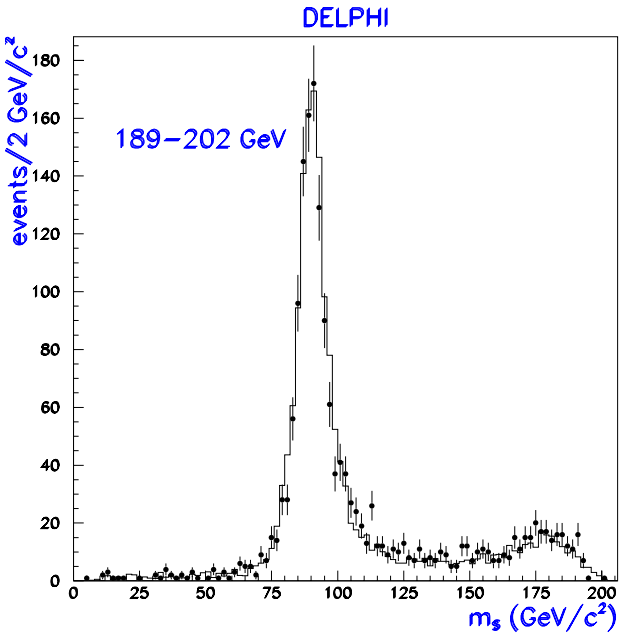

Figure 4: Photon recoil mass spectrum for the γgg candidates (points) and the expected background (histogram).

were studied. No evidence of a signal was found in either channel. Upper limits on $S\gamma$ ($P\gamma$) production in the ($m_S(m_P)$, $\sqrt{F}$) plane were derived.

Acknowledgements

We want to thank F. Zwirner for useful explanations of the theoretical framework and for suggestions for possible experimental investigations. We acknowledge in particular the support of
Austrian Federal Ministry of Science and Traffics, GZ 616.364/2-III/2a/98,
FNRS–FWO, Flanders Institute to encourage scientific and technological research in the industry (IWT), Belgium,
FINEP, CNPq, CAPES, FUJB and FAPERJ, Brazil,
Czech Ministry of Industry and Trade, GA CR 202/96/0450 and GA AVCR A1010521,
Danish Natural Research Council,
Commission of the European Communities (DG XII),
Direction des Sciences de la Matière, CEA, France,
Bundesministerium für Bildung, Wissenschaft, Forschung und Technologie, Germany,
General Secretariat for Research and Technology, Greece,
National Science Foundation (NWO) and Foundation for Research on Matter (FOM), The Netherlands,
Norwegian Research Council,
State Committee for Scientific Research, Poland, 2P03B06015, 2P03B11116 and SPUB/P03/DZ3/99,
JNICT–Junta Nacional de Investigação Científica e Tecnológica, Portugal,
Vedecka grantova agentura MS SR, Slovakia, Nr. 95/5195/134,

Ministry of Science and Technology of the Republic of Slovenia,
CICYT, Spain, AEN96–1661 and AEN96-1681,
The Swedish Natural Science Research Council,
Particle Physics and Astronomy Research Council, UK,
Department of Energy, USA, DE–FG02–94ER40817.

We are also greatly indebted to our technical collaborators and to the funding agencies for their support in building and operating the DELPHI detector, and to the members of the CERN-SL Division for the excellent performance of the LEP collider.

References

[1] P.Fayet, Phys. Lett. **B86** (1979) 272;
J.Ellis, K.Enqvist and D.Nanopoulos, Phys. Lett. **B151** (1985) 357;
D.Dicus, S.Nandi and J.Woodside, Phys. Rev. **D** 43(1991) 2951;
A. Brignole, F. Feruglio and F. Zwirner, Nucl. Phys. B **516** (1998)
(Erratum ibid. B **555** (1999) 653) and references therein.

[2] L3 collab., O. Adriani et al., Phys. Lett. **B297** (1992) 469;
ALEPH collab., R. Barate et al., Phys. Lett. **B420** (1998) 127;
DELPHI collab., P. Abreu et al., CERN-EP-2000-021 to be published in Euro Phys. J. C.

[3] CDF collab.,T. Affolder et al. Phys. Rev. Lett. 85 (2000) 1378.

[4] E. Perazzi, G. Ridolfi and F. Zwirner, Nucl. Phys. **B574** (2000) 3.

[5] DELPHI collab., P.Abreu et al., Nucl. Inst. and Meth. **A378** (1996) 57;
DELPHI collab., P. Aarnio et al., Nucl. Inst. and Meth. **A303** (1991) 233.

[6] DELPHI collab., P. Aarnio et al., Nucl. Phys. **B367** (1991) 511.

[7] P. Chochula et al., Nucl. Inst. and Meth. **A412** (1998) 304.

[8] F.A. Berends and R. Kleiss, Nucl. Phys. B **186** (1981) 22.

[9] DELPHI collab., P.Abreu et al., Phys. Lett.**B462** (1999) 425.

[10] S. Catani et al., Phys. Lett. **B269** (1991) 432.

[11] T. Sjöstrand, Comp. Phys. Comm. **39** (1986) 347;
LU TP 95-20 CERN TH 7112-93 (hep-ph/9508391).

[12] F.A. Berends, R. Pittau and R. Kleiss. Comp. Phys. Comm. **85** (1995) 437.

[13] A.L. Read,*Modified Frequentist Analysis of Search Results (The CLs Method)*, CERN-OPEN-2000-205, pp81-101.

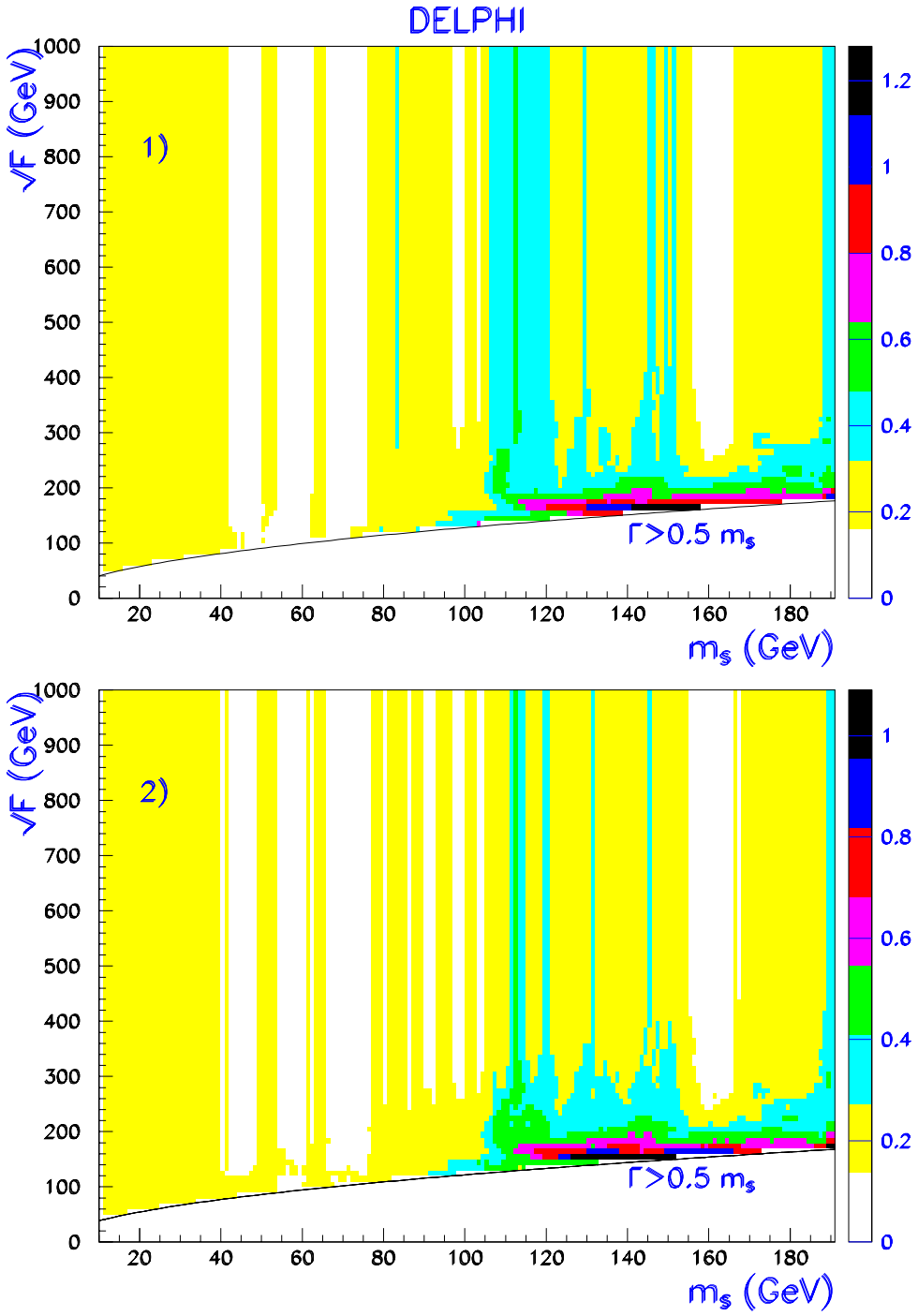

Figure 5: Cross section (pb) upper limit at the 95% Confidence Level as a function of m_S and $\sqrt{F}$ for the two sets of parameters of Tab. 1.

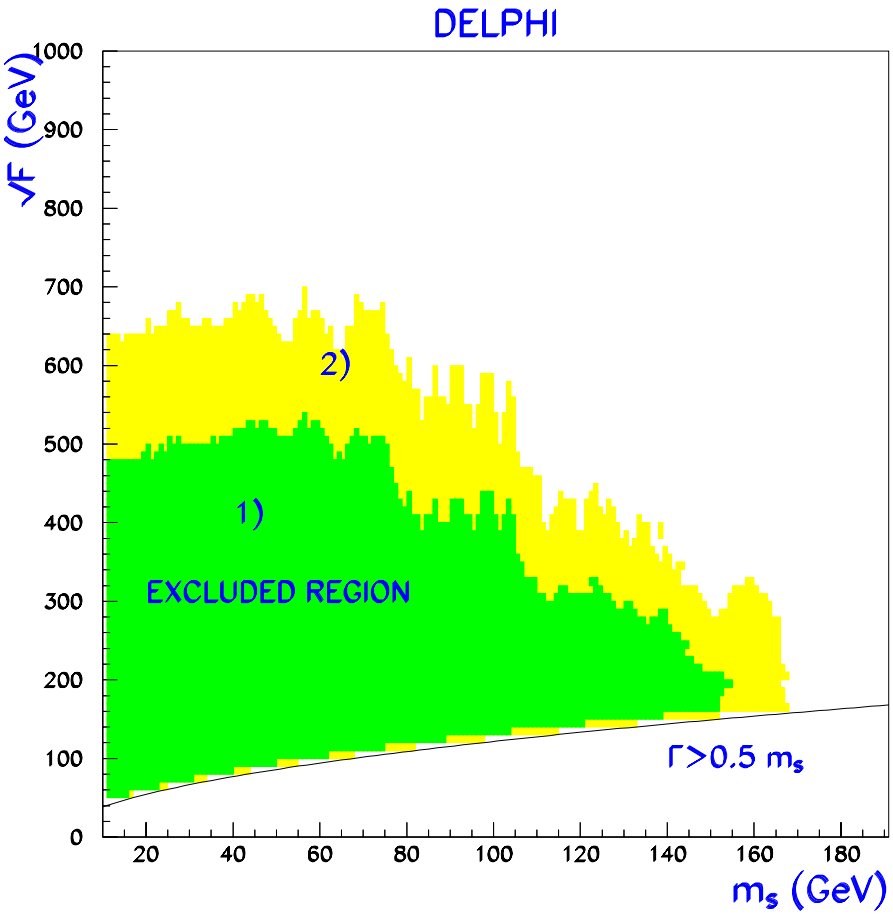

Figure 6: Exclusion region at the 95% Confidence Level in the m_S, $\sqrt{F}$ plane for the two sets of parameters of Tab. 1.

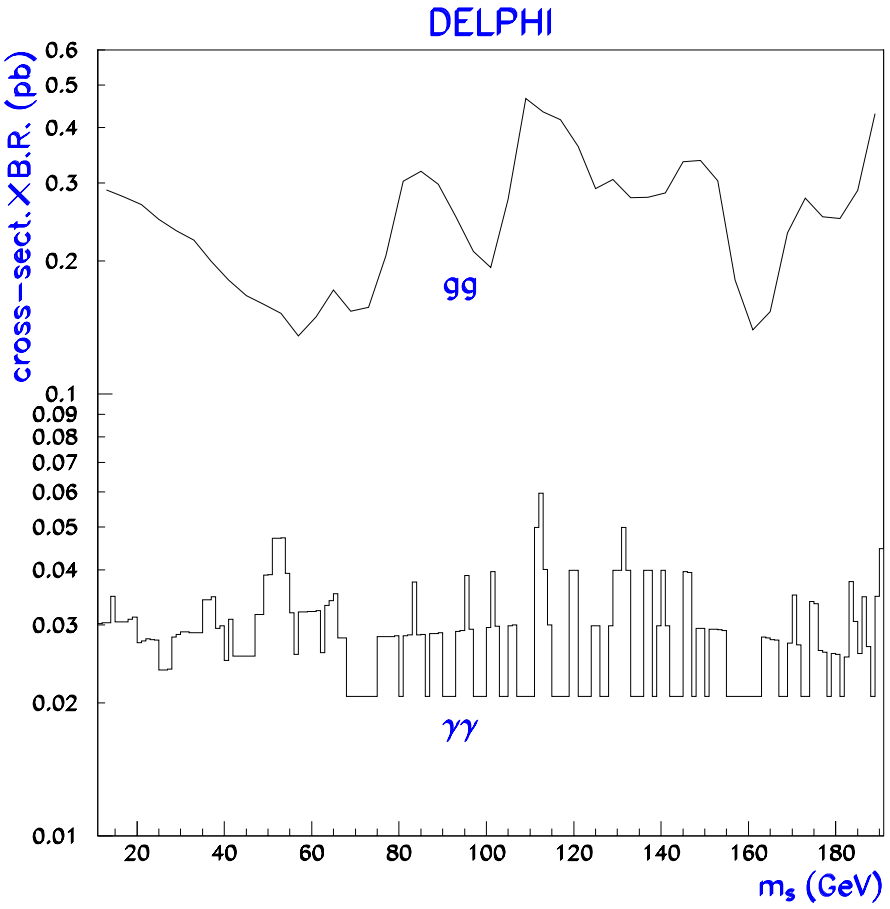

Figure 7: Cross section times branching ratio limits at the 95% Confidence Level for the two decay channels investigated. They are obtained for $\sqrt{F} \geq 500$ GeV, corresponding to the region where the expected signal width is dominated by the experimental resolution. The bin size was chosen to match the experimental mass resolution.